Journal of Information Display
Vol. 12, No. 1, March 2011, 1–4

Taylor & Francis
Taylor & Francis Group

Organic complementary inverter and ring oscillator on a flexible substrate

Mingyu Kim, Hyunduck Cho, Jeonghun Kwak, Chan-mo Kang, Myeong-jin Park and Changhee Lee*

School of Electrical Engineering and Computer Science, Interuniversity Semiconductor Research Center, Seoul National University, South Korea

(*Received 9 September 2010; Revised 5 November 2010; Accepted for publication 5 November 2010*)

A complementary inverter was fabricated using pentacene and N-N′-dioctyl-3,4,9,10-perylene tetracarboxylic diimide-C8 (PTCDI-C8) for p- and n-type transistors on a poly(ether sulfone) substrate, respectively. The mobilities of the p- and n-type transistors were 0.056 and 0.013 $cm^2/V\,s$, respectively. The inverter, which was composed of p- and n-type transistors, showed a gain of 48.6 when $V_{DD} = -40\,V$ and at the maximum noise margin of $V_{DD}/2$. A ring oscillator was also fabricated by cascading five inverters. The five-stage ring oscillator showed the maximum output frequency of 10 kHz when $V_{DD} = -170\,V$.

Keywords: flexible; OTFT; complementary; inverter; oscillator

1. Introduction

Organic field-effect transistors (OFETs) such as flat panel displays [1], flexible sensors [2], and radio frequency identification (RFID) tags have an enormous potential for low-cost, large-area, and flexible electronics [3], for which reason they are attracting much attention. OFET-based inverters and ring oscillators have been studied by many researchers as basic building blocks for complex integrated circuits. At first, researches on unipolar circuits of inverters were actively conducted [4,5] because of the higher hole mobility of organic materials compared to electron mobility. Furthermore, most low-work-function metals as source and drain electrodes for lowering the electron injection barrier are easily oxidized in ambient air. This notwithstanding, complementary circuits made of both n- and p-type transistors have many advantages, such as low power consumption, high noise margin, and robustness. As such, since the release of the initial results of Bell Labs [6], several groups have studied and have reported the results of their researches on complementary OFET circuits [7–9]. In these studies, the photolithography process was used to deposit electrodes. Photolithography has the advantages of narrowing the width of the source and drain electrodes and of minimizing the overlap area between the gate electrode and the source and drain electrodes so that the overlap capacitance can be reduced, but it is difficult to form a top-contact structure using it, and to process it on a flexible plastic substrate.

In this study, source and drain electrodes were fabricated via vacuum deposition, which is a more cost-effective process compared to photolithography. Not only the electrodes but also the active layers were deposited via vacuum deposition, using the following materials. Pentacene, which is well known to have high hole mobility reaching $5.5\,cm^2/V\,s$ [10], was used as the active layer for the p-type transistors in this study, and N-N′-dioctyl-3,4,9,10-perylene tetracarboxylic diimide with eight alkyl chains (PTCDI-C8) was used for the n-type transistors, among some possible n-type materials [11–13].

2. Experiments

All the devices were fabricated with a bottom-gate top-contact structure, as shown in Figure 1. At first, indium-tin-oxide (ITO) gate electrode was deposited on a 2×2-cm poly (ether sulfone) (PES) substrate by sputtering, and the substrate was rinsed with isopropyl alcohol (IPA). Then a dielectric layer was formed by spin-coating poly-4-vinylphenol (PVP, Sigma Aldrich) solution (12 wt%) consisting of PVP, poly(melamine-co-formaldehyde) (PMCF, Sigma Aldrich) cross-linker, and propylene glycol methyl ether acetate (PGMEA, Sigma Aldrich) at the ratio of 12:12/5:100, followed by curing in a vacuum oven at 200 °C for 30 min. The PVP dielectric layer was about 460 nm thick. Subsequently, 60 nm PTCDI-C8 (Sigma Aldrich) and pentacene (Tokyo Chemical Industry) were deposited via thermal evaporation under 1×10^{-6} Torr pressure. PTCDI-C8 was evaporated at a rate of 0.5 Å/s with the substrate temperature of 100 °C, and then pentacene was deposited at a rate of 0.3 Å/s with the substrate

*Corresponding author. Email: chlee7@snu.ac.kr

ISSN 1598-0316 print/ISSN 2158-1606 online

DOI: 10.1080/15980316.2011.555507
http://www.informaworld.com

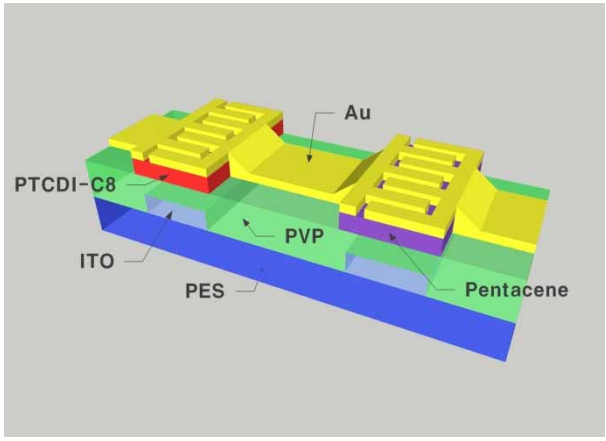

Figure 1. Structure of the complementary inverter.

temperature of 70 °C. At last, source and drain electrodes were formed by evaporating Au onto the active layer at a rate of 1.0–1.5 Å/s. The channel width and length of each transistor were 10,900 and 50 μm, respectively. Especially, the source and drain electrodes were deposited in the form of multifinger electrodes for a wide channel width, which makes a large amount of the current flow at each inverter. Therefore, this makes it possible to drive a large load connected at the output terminal of a ring oscillator rapidly. The characteristics of the transistors and inverters were measured using an HP 4155C semiconductor analyzer, and the output of the ring oscillator was measured using a Tektronix TDS5054B digital oscilloscope with a Keithley 236 source measure unit. All the measurements were performed in a glove box filled with nitrogen gas.

3. Results and discussion

First, the electrical characteristics of pentacene and PTCDI-C8 OFETs were measured to determine the performance of each OFET. The transfer characteristics of the devices were measured while varying the gate voltage (V_G) from 10 to −60 V for the p-type device and from −10 to 60 V for the n-type device at the drain voltage (V_{DD}) of −40 V (or 40 V). The mobilities of the p- and n-type transistors were 0.056 and 0.013 $cm^2/V\,s$, respectively, and their threshold voltages (V_{th}) were −30 and 35 V. The devices showed similar on-off current ratios of 10^5. The transfer curves of both the p- and n-type transistors were nearly symmetric with respect to the axis of $V_G = 0$ V, as shown in Figure 2. Therefore, the level-transition voltage (V_{inv}) can be expressed as the midpoint of V_{DD} according to the following equation [14]:

$$V_{inv} = \frac{V_{DD} + V_{th}^{p} + V_{th}^{n}\sqrt{\beta_n/\beta_p}}{1 + \sqrt{\beta_n/\beta_p}},$$

where V_{th} is the threshold voltage and $\beta = (W/L)\mu C_g$ is a factor for controlling the current of the OFETs. As a result, the noise margin of the inverter was maximized as the value of $V_{DD}/2$. Figure 3 shows these characteristics through the input–output ($V_{IN} - V_{OUT}$) transfer curves and gain curves, depending on the applied bias voltage. The gain of the inverter was about 48 when $V_{DD} = -40$ V, which is large enough for the inverter to be used as a voltage amplifier that can amplify a small signal coupled with a DC voltage of $V_{DD}/2$.

Figure 4(a) shows an image of the five-stage ring oscillator on the flexible PES substrate, and Figure 4(b) shows a schematic diagram of the five-stage ring oscillator, composed of five complementary inverters. The output terminal (V_O) of the last stage is connected to the input terminal (V_I) of the first stage with a feedback line. The output signal observed at V_O started oscillating with the oscillation frequency (f_{OSC}) of 12 Hz when $V_{DD} = -37$ V was applied, and f_{OSC} simultaneously increased when the bias voltage was increased, as plotted in Figure 4(c). Finally, the maximum output frequency reached 10 kHz at $V_{DD} = -170$ V, as shown in Figure 4(d). This value is not higher than the previously reported one [7–9], but it was obtained from devices that were fabricated via photolithography. Although the f_{OSC} value obtained in this work is slightly lower than the previous values obtained, it is noticeable that a high frequency of 10 kHz was achieved when thermal evaporation was performed on the flexible substrate using commercial organic semiconductors. It is thus believed that much higher

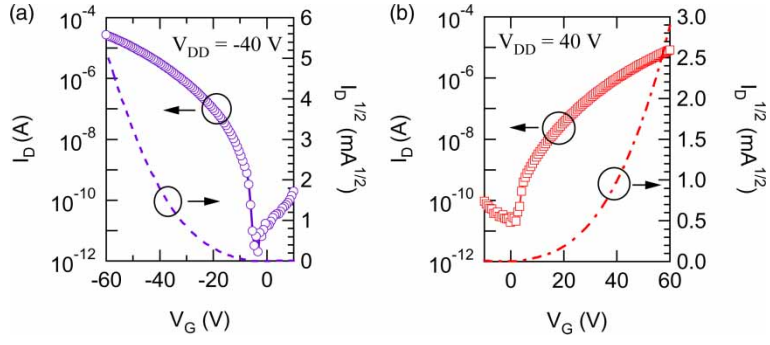

Figure 2. Transfer curves of (a) pentacene and (b) PTCDI-C8 transistors.

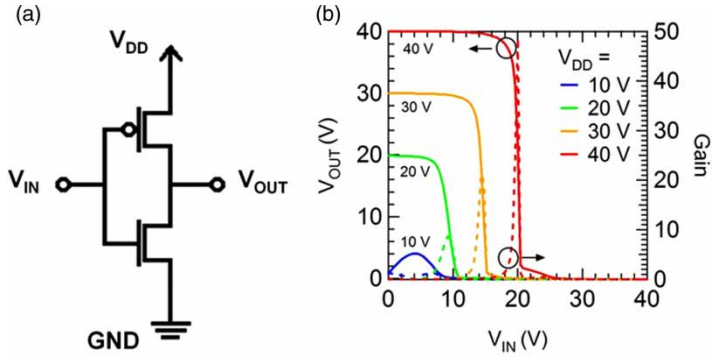

Figure 3. (a) Schematic diagram of a complementary inverter. (b) Output characteristics of the complementary inverter: $V_{IN} - V_{OUT}$ transfer curves (solid line) and gains (dashed line).

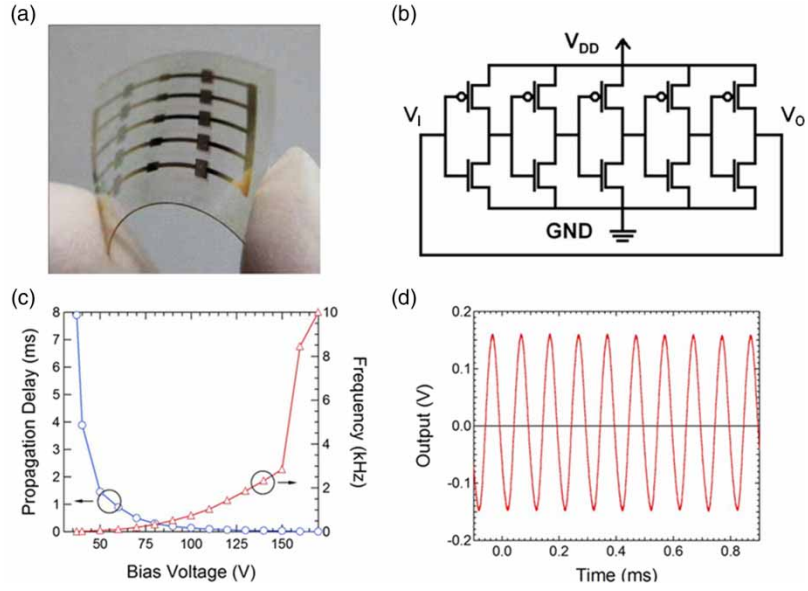

Figure 4. (a) An image of the five-stage ring oscillator on the flexible PES substrate (PES). (b) Schematic diagram of the five-stage ring oscillator. (c) Characteristics of the propagation delay in the one-stage inverter, and output frequency of the ring oscillator versus bias voltage. (d) The output signal of the five-stage ring oscillator at $V_{DD} = -170$ V shows $f_{OSC} = 10$ kHz.

performances of inverters or multistage ring oscillators can be obtained by using better organic semiconductors that possess high mobilities.

4. Summary

Complementary inverters and five-stage ring oscillators were fabricated on flexible substrates based on pentacene and PTCDI-C8 as the p- and n-type active layers, respectively. Both OFETs showed moderate mobilities (i.e. 0.056 and 0.013 $cm^2/V\,s$ for the p- and n-type transistors, respectively) and similar on-off current ratios (about 10^5). The complementary inverters showed good characteristics in terms of gain (ca. 48 at $V_{DD} = -40$ V) and maximum noise margin ($V_{DD}/2$). The five-stage ring oscillator started oscillating from the bias voltage of -37 V, and it showed the highest oscillating frequency of 10 kHz at $V_{DD} = -170$ V. The results presented in this paper are noteworthy as high-frequency operation was achieved by using thermal evaporation on a flexible substrate with typical organic semiconductors. It also shows that OFETs can be used in digital integrated circuits.

Acknowledgements

This work was supported by the IT R&D Program of MKE/KEIT [10030559, Development of Next-Generation High-Performance Organic/Nano Materials and Printing Process Technology].

References

[1] G.H. Gelinck, H.E.A. Huitema, E. van Veenendaal, E. Cantatore, L. Schrijnemakers, J.B.P.H van der Putten, T.C.T.

Geuns, M. Beenhakkers, J.B. Giesbers, B.H. Huisman, E.J. Meijer, E.M. Benito, F.J. Touwslager, A.W. Marsman, B.J.E. van Rens, and D.M. de Leeuw, Nat. Mater. **3**, 106 (2004).

[2] J.B. Chang, V. Liu, V. Subramanian, K. Sivula, C. Luscombe, A. Murphy, J. Liu, and J.M.J. Frechet, J.Appl. Phys. **100**, 014506 (2006).

[3] E. Cantatore, T. Geuns, A. Gruijthuijsen, G. Gelinck, S. Drews, and D.M. de Leeuw, Dig. Tech. Pap.-IEEE Int. Solid-State Circuits Conf. **49**, 273 (2006).

[4] H. Klauk, M. Kalik, U. Zschieschang, F. Eder, G. Schmid, and C. Dehm, Appl. Phys. Lett. **82**, 4175 (2003).

[5] P.F. Baude, D.A. Ender, M.A. Haase, T.W. Kelley, D.V. Muyres, and S.D. Thesiss, Appl. Phys. Lett. **82**, 3964 (2003).

[6] B. Crone, A. Dodalbalapur, Y.-Y. Lin, R.W. Filas, Z. Bao, A. LaDuca, R. Sarpeshkar, H.E. Katz, and W. Li, Nature **403**, 521 (2000).

[7] H. Klauk, M. Kalik, U. Zschieschang, F. Eder, D. Rohde, G. Schmid, and C. Dehm, IEEE Trans. Electron Dev. **52**, 618 (2005).

[8] B. Yoo, T. Jung, D. Basu, and A. Dodabalapur, Appl. Phys. Lett. **88**, 082104 (2006).

[9] D. Bode, K. Myny, B. Verreet, B. van der Putten, P. Bakalov, S. Steudel, S. Smout, P. Vicca, J. Genoe, and P. Heremans, Appl. Phys. Lett. **96**, 133307 (2010).

[10] S. Lee, B. Koo, J. Shin, E. Lee, H. Park and H. Kim, Appl. Phys. Lett. **88**, 162109 (2006).

[11] S. Tatemichi, M. Ichikawa, S. Kato, T. Koyama, and Y Taniguchi, Phys. Stat. Sol. **2**, 49 (2008).

[12] S. D. Vusser, S. Steudel, K. Myny, J. Genoe, and P. Heremans, Appl. Phys. Lett. **88**, 162116 (2006).

[13] J. Jang, J. W. Kim, N. Park, and J. Kim, Org. Electron. **9**, 481 (2008).

[14] T. A. DeMassa and Z. Cicone, in *Digital Integrated Circuits* (Wiley, New York, 1996), p. 342.

[Part of this work was presented in International Workshop on Flexible & Printable Electronics 2010 (IWFPE 2010).]